

Molecular Frame Photoelectron Emission in the Presence of Autoionizing Resonances

M. Lebech,^{1,*} J. C. Houver,¹ D. Dowek,¹ and R. R. Lucchese²

¹*Laboratoire des Collisions Atomiques et Moléculaires (LCAM, UMR Université Paris Sud et CNRS, No. 8625),
Bâtiment 351, Université Paris Sud, F-91405 Orsay Cedex, France*

²*Department of Chemistry, Texas A&M University, College Station, Texas 77843-3255, USA*

(Received 12 July 2005; published 22 February 2006)

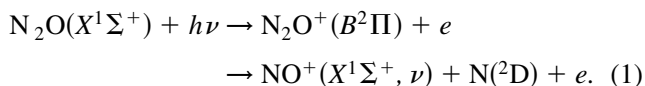
We have measured the angular distribution of valence-shell photoelectrons excited by circularly polarized light from fixed-in-space N₂O molecules, near to and on top of resonances due to Rydberg states embedded in the ionization continuum. The sign of the circular dichroism for ionization into the N₂O⁺(B²Π, (1π)⁻¹) state is reversed on top of the lowest dominant resonances. Measured angular distributions are well predicted by state-of-the-art multichannel configuration interaction calculations. The change in sign of the circular dichroism at the peak of the resonance is the result of a rapid change in the phases of resonant dipole matrix elements by a factor of 2π as the energy is scanned across the resonance.

DOI: 10.1103/PhysRevLett.96.073001

PACS numbers: 33.80.Eh

One of the fundamental features of quantum mechanics is the superposition principle which can lead to quantum interference effects. For states in the ionization continuum of molecules the wave functions of physical scattering states are necessarily complex valued. Measuring molecular frame photoelectron angular distributions (MFPADs) induced by circularly polarized light gives the most complete access to these phases [1–4]. These observables can exhibit dramatic interference effects in the region of narrow resonances due to rapidly changing values of the quantum phases.

In this study, we show the influence of such interference effects on MFPADs in the resonant autoionization of Rydberg states embedded in the continuum of the N₂O molecule. We report angular distribution of (1π)⁻¹ valence shell photoelectrons excited by circularly polarized light from fixed-in-space N₂O molecules in the 18–22 eV region where both direct ionization (DI) and resonant autoionization (AI) of Rydberg states populate the B²Π(1π)⁻¹ ionic state, leading to dissociative photoionization (DPI) according to the reaction:



Four Rydberg series converging to the C²Σ⁺ electronic state of N₂O⁺ were first observed in photoabsorption [5], and assigned as *npσ*, *npπ*, *ndσ*, and *ndπ* by Lindholm [6]. A fifth series close to the *ndπ* series was assigned to *nsσ* by high resolution mass spectrometry [7]. The influence of these resonant states has been observed in other competing decay processes such as neutral dissociation [8], and ion-pair formation [9]. No theoretical description of these autoionization processes has been previously given.

Taking advantage of the DPI process Eq. (1), we have measured the MFPADs using the vector correlation approach combined with circularly polarized light [1]. In the 18–22 eV explored energy region, two-dimensional

photoelectron spectroscopy [10], recording the electron yield as a function of both electron and photon energy, showed that the dominant contribution to autoionization into the N₂O⁺(B²Π) ionic state arises from the decay of the two series assigned as *ndπ* and *nsσ*. We therefore selected three photon energies [*hν* = 18.55, 19.25, and 19.56 eV [7,10]] in order to probe AI on top of the most prominent Rydberg states assigned as *ndπ* (*n* = 3, 4, 5), and a few other off-resonance values as a probe of DI at neighboring photon energies (see inset of Fig. 3).

To our knowledge, these results represent the first case where circular dichroism of electron emission in the molecular frame has been used as a probe of the excitation of autoionizing states. Angle resolved photoelectron spectroscopy for studying the dynamics of autoionization has been applied in a few recent studies of vibrational autoionization of Rydberg states of NO [11] and electronic autoionization of O₂ [12,13] and H₂ [14] induced by linearly polarized light. In the present study, experimental results, compared with multichannel Schwinger configuration interaction (MCSCI) calculations, demonstrate the sensitivity of the MFPADs to the photoionization dynamics due to the presence of autoionizing resonances. They also suggest a re-assignment of the dominant autoionizing Rydberg series in this region.

The (**V**_{NO⁺}, **V**_e, **ê**) vector correlation method consists here of measuring for each DPI event the three components of the **V**_{NO⁺} ion fragment and **V**_e photoelectron nascent velocity vectors, deduced from the arrival time and position of both particles in the double velocity spectrometer described in detail previously [15]. Briefly, the interaction region is defined at the intersection of a supersonic molecular beam [16] and the circularly polarized light beam delivered by SU5 undulator-based vacuum ultraviolet beam line [17] at Super-ACO, operated in the two-bunch mode. Ions and electrons are extracted from the interaction region by a dc electric field **E** whose magnitude ensures a 4π collection of both particles, and guided to the two

position sensitive detectors through an intermediate region where focusing lens sets are set to control the trajectories [15]. The circular polarization rate s_3/s_0 of the light was controlled to be higher than 0.95.

In a detailed study of reaction Eq. (1) using linearly polarized light, and focused on DI [18], we have shown how the DPI events can be conveniently selected using the electron-ion kinetic-energy correlation. The angular analysis established that DI into the $B^2\Pi$ state corresponds to a dominant perpendicular transition ($\beta_{\text{NO}^+} \approx -0.2$), and suggested that a significant bending of the N_2O molecule occurs prior to dissociation of that ionic state.

For the data reported presently, the MFPADs are deduced from the analysis of the $(\mathbf{V}_{\text{NO}^+}, \mathbf{V}_e, \hat{\mathbf{e}})$ vector correlation for the events selected as described in Ref. [18], after a three angle fit of the $I(\chi, \theta_e, \phi_e)$ distribution, which can be written as

$$\begin{aligned} I_{+1}(\chi, \theta_e, \phi_e) = & F_{00}(\theta_e) - 0.5F_{20}(\theta_e)P_2^0(\cos\chi) \\ & - 0.5F_{21}(\theta_e)P_2^1(\cos\chi)\cos(\phi_e) \\ & - 0.5F_{22}(\theta_e)P_2^2(\cos\chi)\cos(2\phi_e) \\ & + F_{11}(\theta_e)P_1^1(\cos\chi)\sin(\phi_e) \end{aligned} \quad (2)$$

for a left-handed circularly polarized light (helicity +1). χ is the polar angle of the molecular axis with respect to the light propagation axis \mathbf{y} , and (θ_e, ϕ_e) defines the electron emission in the molecular frame. Such a general expression has the great advantage of disentangling the photoionization dynamics information by expressing the MFPADs for any chosen orientation of the molecular axis with respect to the light axis [1] in terms of five $F_{LN}(\theta_e)$ functions (four functions for a linear polarization), where the dependence on ϕ_e and χ is through low order analytical functions. For the (NO^+, e) coincident events considered in Eq. (1), θ_e is the polar angle with respect to the \mathbf{z}_{MF} N_2O molecular axis oriented with the O end in the positive direction, and $\phi_e = 0^\circ$ corresponds to electron emission in the $y > 0$ ($\mathbf{z}_{\text{MF}}, \mathbf{y}$) half plane.

The F_{11} term in Eq. (2) is proportional to the molecular frame circular dichroism in photoelectron angular distribution (CDAD). The dimensionless CDAD, defined in Eq. (3) for a molecule oriented perpendicular to the \mathbf{y} axis ($\chi = 90^\circ$), and electron emission in the plane perpendicular to \mathbf{y} ($\phi_e = 90^\circ$ and 270°), is obtained in an experiment using the light of a single helicity (here +1), as [19]

$$\text{CDAD} = \frac{I_{\phi_e=90} - I_{\phi_e=270}}{I_{\phi_e=90} + I_{\phi_e=270}} = \frac{2F_{11}}{2F_{00} + \frac{1}{2}F_{20} + 3F_{22}}. \quad (3)$$

The F_{LN} functions for Eq. (1) were computed using nearly the same calculation as discussed in Ref. [18]. We use the MCSCI method [20] in which the initial and final bound state wave functions are described using configuration interaction (CI) wave functions. The expansion of the photoionized continuum state was restricted to the $X^2\Pi$,

$A^2\Sigma^+$, $B^2\Pi$, and $C^2\Sigma^+$ ion states. The correction required since Eq. (1) does not satisfy the axial recoil approximation involves a recoil angle, i.e., the angle between the asymptotic velocity of the recoil fragments and the original molecular axis, of $\theta_R = 30^\circ$ [18]. It is included when comparing the measured and computed MFPADs.

In Fig. 1(a) we display the newly measured F_{11} function for the DI component of the DPI process described in Eq. (1) at 19.5 eV photon energy; the other four F_{LN} functions have been reported previously in Ref. [18]. For DI in the $\text{N}_2\text{O}^+(B^2\Pi)$ state, F_{11} varies smoothly as the photon energy is scanned from the ionization threshold to 2 eV above threshold. The measured F_{11} function shows a single positive oscillation for all nonresonant DI energies explored. At the angle where the maximum amplitude of F_{11} occurs, the measured CDAD parameter is ~ 0.2 . This value is smaller than that measured recently in outer shell [1,2,19] and inner shell [3] photoionization. In Fig. 1(b) we plot the cut of the MFPAD in the polarization plane of circularly polarized light of helicity +1, for a molecule oriented perpendicular to the \mathbf{y} axis. This polar angle distribution, which is the most appropriate for visualization of the circular dichroism, is simply obtained from the general expression in Eq. (2) as

$$I_{+1, \chi=90, \phi_e=90/270} = F_{00} - 0.5F_{20} - 1.5F_{22} \pm F_{11}. \quad (4)$$

The shape of the measured MFPAD is rather smooth; however, the favored electron emission in the half plane $\phi_e = 90^\circ$ for Eq. (1) illustrates the positive circular dichroism.

The first set of MCSCI calculations presented in Fig. 1 (full line) corresponds to the calculated MFPADs for DI in Eq. (1), as described above. F_{11} for DI into the $\text{N}_2\text{O}^+(B^2\Pi)$ state shows pronounced oscillations, smoothly evolving for the four explored nonresonant energies. The CDAD oscillates between 1 and -1 for Eq. (1), indicating a strong MF circular dichroism. The second set of computed F_{11} functions and MFPADs (dashed line) takes into account the mean $\theta_R = 30^\circ$ recoil angle [18]. Including this correction significantly decreases the appar-

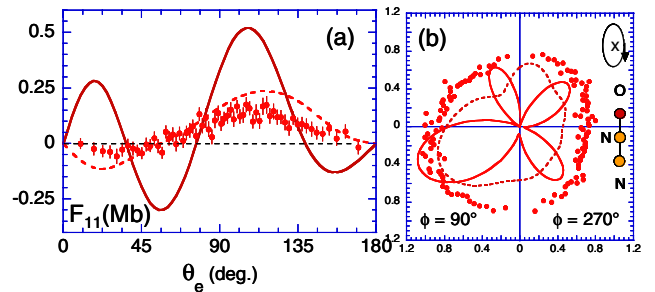


FIG. 1 (color online). The F_{11} function for DI Eq. (1) (a) and the related cut of the MFPAD induced by LHC light (b) (see text) at $h\nu = 19.5$ eV. Dots: experiment; full line: calculations; dashed line: calculations corrected for bending. Theory and experiment are normalized such that the total DI cross sections are identical.

ent CDAD, leading to a very good agreement between the measured and calculated F_{11} functions. The agreement is less satisfactory at the level of the MFPAD: this is mainly due to the difference between the measured and calculated F_{22} functions at this energy discussed previously [18].

Figures 2(a)–2(e) display the five F_{LN} functions measured for Eq. (1) on top of the lowest resonance at 18.55 eV previously assigned as $3d\pi$. Two features are clearly different from those observed for DI at neighbor energies. (i) The negative sign of F_{11} , also measured at 19.25 eV, indicates that the positive CDAD which characterizes DI into the B state (see Fig. 1) is reversed on top of the resonance. (ii) The positive sign of F_{20} indicates a positive asymmetry parameter $\beta_{\text{NO}^+} \approx 0.45 \pm 0.1$, i.e., a dominant parallel transition, although DI into the B state corresponds to a dominant perpendicular transition [18]. A similar trend is found at the corresponding Rydberg autoionization resonances at 19.25 eV, and to a lesser extent at 19.56 eV, which suggests that the resonant states in this series have a σ symmetry. The calculations also support the assignment of the σ character of the dominant Rydberg series in the sense that the larger and broader resonant structures correspond to σ states, although the positions are shifted relative to those found in the experiment. In order to compare the computed and experimental MFPADs of the AI reso-

nances, we have adjusted the energy of the resonances so that their positions agree with the values determined experimentally and the Coulomb phase shift of the computed matrix elements to the corresponding experimental photoelectron kinetic energies. Since ionization occurs through the B state, the same mean recoil angle of $\theta_R = 30^\circ$ as for DI is included in the calculation of the F_{LN} functions; finally, a bandwidth of 25 meV is introduced to account for the measured energy width at the resonance peak. The comparison between the measured F_{LN} functions and those computed for the σ resonant state is quite satisfactory and support this symmetry assignment. In particular the reversed CDAD is very well predicted; the main discrepancies concern the F_{22} functions, as previously found for DI, and the rise of the computed F_{00} and F_{20} as $\theta_e \rightarrow 180^\circ$.

The value of the F_{11} function results from the coherent superposition of photoelectrons produced by light polarized parallel and perpendicular to the molecular axis. Its explicit expression is a sum of products of dipole matrix elements for the parallel and perpendicular transitions. In the region of an autoionization resonance, the phases of the matrix elements from one of these symmetries will change rapidly; for the system considered here these are the matrix elements for parallel ionization. In general, in the region of a narrow scattering resonance, the scattering phase shift will rise, as a function of energy, by π radians. This change in scattering phase will also change the phase of the dipole matrix elements in photoionization, which leads to a rise of π radians in the case of shape resonances [1]. However, in the case of autoionization, there is an additional phase change of π radians since the resonant part of the cross section goes through zero in such a resonance [21]. The net effect is that the matrix element phases change by even multiples of π (i.e., $0, \pm 2\pi$) as the energy passes through an autoionization resonance. This energy dependence is explicitly seen in the computed matrix elements in agreement with the experimental results obtained before, on top

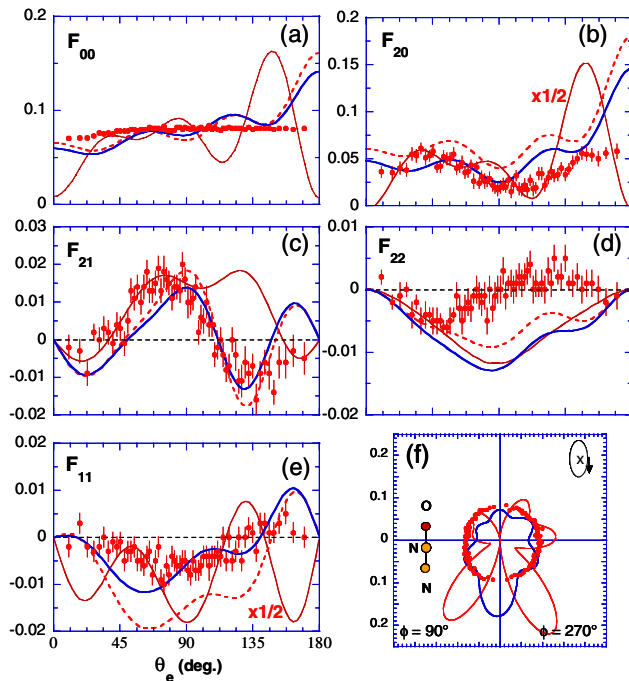


FIG. 2 (color online). The F_{LN} functions (a)–(e) and the related cut of the MFPAD (f) induced by LHC light measured at 18.55 eV for Eq. (1). Dots: experiments; thin line (red): calculations; dashed line: calculations corrected for bending; thick line (blue): calculations corrected for bending assuming a $w = 25$ meV width. These data are normalized to the same total cross section equal to 1: the absolute values are obtained by scaling the y axis by 33.798 Mb ($w = 0$) and 23.011 Mb ($w = 25$ meV), respectively.

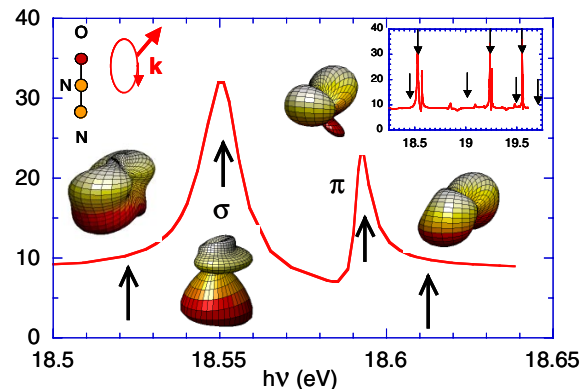


FIG. 3 (color online). Evolution of the computed MFPAD for the N_2O molecule oriented perpendicular to the light propagation axis as shown, nearby and on top of the lowest σ and π resonances. The inset displays the computed photoionization cross section for reaction (1), where the dark arrows indicate the experimentally studied energies.

of, and after the resonance. The dramatic change of F_{11} at the peak of the autoionization resonance and the resumption of the original form after the resonance is thus a consequence of this rapid change in phase of the dipole matrix elements. Figure 3 illustrates the drastic evolution of the computed MFPADs along the lowest set of σ and π resonances in the 18.5 eV region for a molecule oriented perpendicular to the axis of LHC polarized light.

In conclusion, we have reported experimental and theoretical MFPADs for photoionization of the N_2O molecule induced by circularly polarized light at photon energies where both DI and AI of Rydberg states contribute to the production of the $B^2\Pi$ state of N_2O^+ . These MFPADs constitute a very sensitive probe of the AI process: in particular, the positive CDAD for DI into the $B^2\Pi$ state is reversed on top of the lowest resonances. This is due to the fact that the phase of dipole matrix elements change by even multiples of π (i.e., $0, \pm 2\pi$) as the energy passes through the resonance. The MFPAD results suggest that the dominant Rydberg series converging to the C state has σ symmetry. The MCSCI calculations are in very good agreement with the measurements for the dominant features; however, the energy width of the measured resonant peaks as well as some features of the MFPADs are not well predicted yet. Further experiments are planned to probe the evolution of the MFPADs along the σ and π resonances, as displayed in Fig. 3 for the calculations, using high energy resolution third generation synchrotron radiation.

We are very grateful to L. Nahon, SU5 beam line scientist, and to B. Pilette at LURE for his technical assistance. The support of the National Science Foundation through Grant No. INT-0089831, the Welch Foundation under Grant No. A-1020, and the Centre de la Recherche Scientifique is gratefully acknowledged.

*Present address: Photon Factory, 1-1 Oho, Tsukuba, Ibaraki 305-0801, Japan.

- [1] M. Lebech, J.C. Houver, A. Lafosse, D. Dowek, C. Alcaraz, L. Nahon, and R.R. Lucchese, *J. Chem. Phys.* **118**, 9653 (2003), and references therein.
- [2] O. Gessner, Y. Hikosaka, B. Zimmermann, A. Hempelmann, R.R. Lucchese, J.H.D. Eland, P.M. Guyon, and U. Becker, *Phys. Rev. Lett.* **88**, 193002 (2002).
- [3] T. Jahnke *et al.*, *Phys. Rev. Lett.* **88**, 073002 (2002).
- [4] S. Motoki, J. Adachi, K. Ito, K. Ishii, K. Soejima, A. Yagishita, S.K. Semenov, and N.A. Cherepkov, *Phys. Rev. Lett.* **88**, 063003 (2002).
- [5] Y. Tanaka, A.S. Jursa, and F.J. Leblanc, *J. Chem. Phys.* **32**, 1205 (1960).
- [6] E. Lindholm, *Ark. Fys.* **40**, 129 (1969).
- [7] J. Berkowitz and J.H.D. Eland, *J. Chem. Phys.* **67**, 2740 (1977).
- [8] M. Ukai, K. Kameta, S. Machida, N. Kouchi, Y. Hatano, and K. Tanaka, *J. Chem. Phys.* **101**, 5473 (1994).
- [9] K. Mitsuke, S. Suzuki, T. Imamura, and I. Koyano, *J. Chem. Phys.* **92**, 6556 (1990).
- [10] E. Sokell, A.A. Wills, J. Comer, and P. Hammond, *J. Phys. B* **30**, 2635 (1997).
- [11] J. Guo, A. Mank, and J.W. Hepburn, *Phys. Rev. Lett.* **74**, 3584 (1995); H. Park, I. Konen, and R.N. Zare, *Phys. Rev. Lett.* **84**, 3819 (2000).
- [12] A.V. Golovin, F. Heiser, C.J.K. Quayle, P. Morin, M. Simon, O. Gessner, P.M. Guyon, and U. Becker, *Phys. Rev. Lett.* **79**, 4554 (1997).
- [13] A. Lafosse, J.C. Brenot, P.M. Guyon, J.C. Houver, A.V. Golovin, M. Lebech, D. Dowek, P. Lin, and R.R. Lucchese, *J. Chem. Phys.* **117**, 8368 (2002).
- [14] A. Lafosse, M. Lebech, J.C. Brenot, P.M. Guyon, L. Spielberger, O. Jagutzki, J.C. Houver, and D. Dowek, *J. Phys. B* **36**, 4683 (2003).
- [15] M. Lebech, J.C. Houver, and D. Dowek, *Rev. Sci. Instrum.* **73**, 1866 (2002), and references therein.
- [16] M. Richard-Viard, A. Delboulb , and M. Vervloet, *Chem. Phys.* **209**, 159 (1996).
- [17] L. Nahon and C. Alcaraz, *Appl. Opt.* **43**, 1024 (2004).
- [18] M. Lebech, J.C. Houver, D. Dowek, and R.R. Lucchese, *J. Chem. Phys.* **120**, 8226 (2004).
- [19] D. Dowek, M. Lebech, J.C. Houver, and R.R. Lucchese, *J. Electron Spectrosc. Relat. Phenom.* **141**, 211 (2004).
- [20] R.E. Stratmann, R.W. Zureski, and R.R. Lucchese, *J. Chem. Phys.* **104**, 8989 (1996).
- [21] U. Fano, *Phys. Rev.* **124**, 1866 (1961).